

HYDROGEN ADSTATES IN SUBSTITUTED Fe-Ti INTERMETALLICS; A TDS STUDY

N.M. GUPTA, V.S. KAMBLE, S.K. KULSHRESHTHA and R.M. IYER

Chemistry Division, Bhabha Atomic Research Centre, Bombay - 400 085, India

Received 1 February 1989; accepted 7 April 1989

Hydrogen adstates in FeTi intermetallics have been investigated using thermal desorption spectroscopy. The number of adstates and the amount of adsorbed hydrogen was found to increase considerably with increase in titanium content and on substituting iron with manganese while the substitution of iron with nickel had a negligible effect. The desorption peaks observed in the temperature range 300–750 K are attributed to hydrogen adsorbed over Fe/TiO_x or Fe/MnO_x type surface species while the higher temperature peaks are ascribed to H₂ release from FeTi bulk.

1. Introduction

In an earlier paper [1] we have reported on the carbon monoxide methanation activity of FeTi_(1+x) intermetallics ($0 \leq x \leq 0.15$), which are well known hydrogen storage materials [2]. The titanium rich samples, having higher adsorptivity for hydrogen, were found to have higher activity for CO disproportionation and its methanation. A partial replacement of Fe by Mn and that of Ti by Sn is known to result in better activation behaviour [3–5] and such samples have been found to show enhanced activity for CO methanation [6]. The catalytic activity of these materials has been attributed to surface iron clusters, presence of which was demonstrated by us using conversion electron Mössbauer spectroscopy [1].

In continuation of the CO hydrogenation study, we have now investigated hydrogen adsorption/dissociation states over Fe-Ti intermetallics using thermal desorption spectroscopy (TDS). The effect of excess titanium and that of substituting Fe with Mn or Ni on hydrogen adsorption properties has been evaluated.

2. Methods

MATERIALS:

FeTi_(1+x) ($x \leq 0.15$), Fe_{1-x}Mn_xTi ($x \leq 0.3$) and Fe_{1-x}Ni_xTi ($x \leq 0.4$) samples used in this study were prepared by repeated arc melting, as has been described

earlier [1]. The samples were crushed and the 150–300 mesh fraction used for TDS studies had a BET surface area of about $0.5 \text{ m}^2 \text{ g}^{-1}$.

THERMAL DESORPTION SPECTROSCOPY

The hydrogen desorption spectra were recorded under helium carrier flow using 2 g of the sample. The TDS instrument consisted of a stainless steel tubular reactor surrounded with a temperature programmed furnace and is described elsewhere in detail [7]. The bed length of the packed catalyst samples was about 8–9 mm. The inlet to the catalytic reactor was connected to a gas multifold system using which purified He or H_2 could be introduced. The helium purification system consisted of a deoxo catalyst column connected in series with a zeolite and a silica gel trap. The unchanged silica gel colour confirmed that no moisture was carried with He. The effluent gases from the catalytic reactor were analysed with a thermal conductivity detector. Before recording a TDS profile, the samples were treated in flowing hydrogen (50 ml min^{-1}) at 625 K for 3 h and then cooled to room temperature under hydrogen flow. The pressure inside the reactor was around 1.2 atmosphere. The hydrogen was then replaced by helium carrier flow (50 ml min^{-1}) and after equilibrating under He at 298 K, the sample was heated upto 1150 K at a rate of 0.5 K per second.

The activation energy values were estimated using expression $E_d = 2.303RT_m \cdot (2 \log T_m - \log \beta)$ where β and R represent heating rate (s^{-1}) and gas content respectively. This expression has been derived from the equation proposed by Cvetanovic and Amenomiya [8] considering the frequency factor (γ) to be large ($\sim 10^{13} \text{ s}^{-1}$) and neglecting a term $\log(E_d/\gamma R)$ appearing with minus sign at the right hand side of the above expression. The diffusion effect on E_d values was considered negligible due to the non-porous nature of the sample as is indicated by surface area measurement.

3. Results

FeTi SAMPLES

Figure 1 shows TDS profiles from $\text{FeTi}_{(1+x)}$ samples where x varied between 0 and 0.15. TDS profile from FeTi consisted of two broad and overlapping peaks with temperature maxima (T_m) centred at around 660 and 880 K, marked as peaks I and II. The activation energy values (E_d) corresponding to these desorption peaks were estimated to be 75.6 and 105 kJ mol^{-1} respectively. The increase in titanium content considerably affected TDS profiles. Firstly, the temperature of peak I shifted progressively to lower values with increasing Ti content. For the values of $x = 0, 0.05, 0.1$ and 0.15, the temperature of peak I was found to be 660, 530, 500 and 480 K respectively. Secondly, the titanium rich

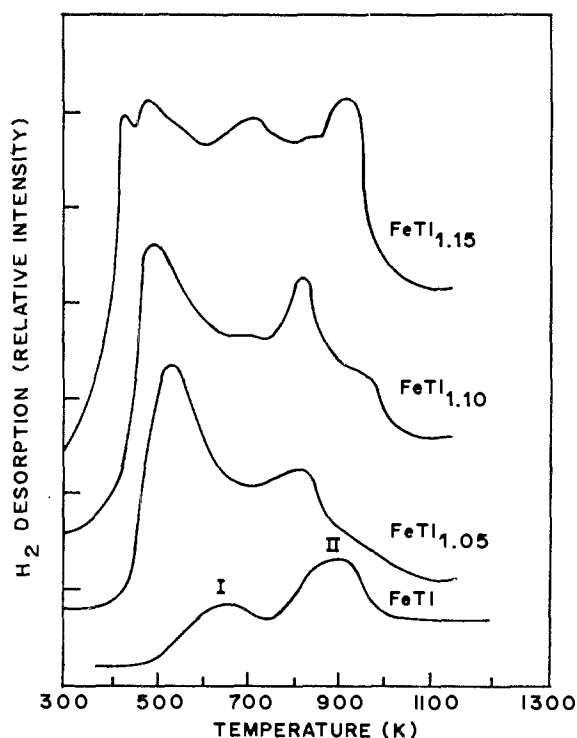


Fig. 1. Hydrogen desorption spectra from FeTi_{1+x} intermetallics having different titanium contents.

samples gave additional peaks in TDS profiles, the spectrum being most complex in case of $\text{FeTi}_{1.15}$ (fig. 1d) which showed desorption peaks with T_m at around 480, 700, 850 and 930 K, corresponding activation energy values being 52.3, 80.7, 100.8 and 111.7 kJ mol^{-1} respectively. This indicated early that in addition to modifying existing adstates, additional H_2 adsorption sites are generated in

Table 1

Thermally desorbed H_2 from FeTi samples of different composition following hydrogen activation at 625 K and 1.2 atm pressure.

Sample composition	H_2 desorbed (ml g^{-1})
FeTi	2.3
$\text{FeTi}_{1.05}$	5.6
$\text{FeTi}_{1.10}$	7.9
$\text{FeTi}_{1.15}$	13.5
$\text{Fe}_{0.9}\text{Mn}_{0.1}\text{Ti}$	39.0
$\text{Fe}_{0.8}\text{Mn}_{0.2}\text{Ti}$	17.5
$\text{Fe}_{0.7}\text{Mn}_{0.3}\text{Ti}$	13.5
$\text{Fe}_{0.9}\text{Ni}_{0.1}\text{Ti}$	3.5
$\text{Fe}_{0.6}\text{Ni}_{0.4}\text{Ti}$	5.0

excess titanium containing samples. The third noticeable aspect of these data is the increase in amount of adsorbed/desorbed H_2 with increasing value of x . The total amount of released hydrogen as evaluated from the area under different profiles is given in table 1.

To evaluate any redistribution or diffusion of hydrogen from one adsite to the other and also to discern individual adsorption sites, a method of partial detrapping prior to the recording of a TDS profile was adopted. In this method, subsequent to room temperature hydrogen adsorption and equilibration in He as mentioned earlier, the sample was heated to a temperature so as to only partially release adsorbed hydrogen and was then cooled to room temperature. The sample was again maintained in He flow for 5 to 6 h before recording the desorption spectrum. Consecutive desorption profiles from a sample were thus obtained by each time increasing the pretreatment temperature. Figures 2(a,b) show consecutive TDS profiles from a $FeTi_{1.15}$ sample recorded 5 h after giving thermal treatment at 575 and 700 K respectively. It may be observed that the hydrogen contributing to higher temperature peaks does not diffuse with time to those sites which give rise to low temperature peaks even though the low temperature sites are rendered vacant by predesorption treatment. The data in fig. 2 also confirm that the broad spectra in fig. 1 indeed constitute several overlapping peaks revealing the existence of a number of distinct and energetically heterogeneous adsites.

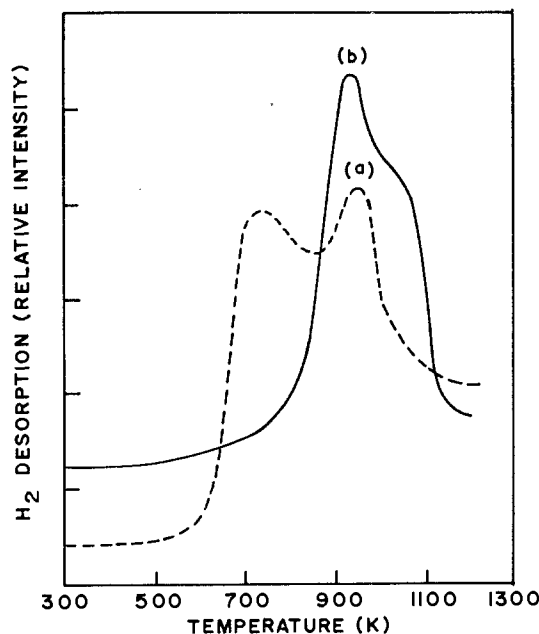


Fig. 2. Effect of thermal pretreatment on desorption spectra of hydrogen recorded consecutively on a $FeTi_{1.15}$ sample. Thermal pretreatment following room temperature H_2 adsorption and prior to starting programmed heating for (a) at 575 K and (b) 700 K.

Mn AND Ni SUBSTITUTED SAMPLES

Figures 3 and 4 show TDS spectra when iron in FeTi was substituted with varying amounts of Mn and Ni respectively. The substitution of Fe with Mn gave rise to intense hydrogen desorption spectra. Curve a of fig. 3 shows the desorption spectrum from a $\text{Fe}_{0.9}\text{Mn}_{0.1}\text{Ti}$ sample where closely spaced and overlapping peaks with maxima at around 500, 550, 750, 875 and 950 K may be identified. Corresponding activation energy values were estimated to be 55, 61.3, 87.5, 104.3 and 114.6 kJ mol^{-1} respectively. With increasing manganese content, a quenching effect was observed as is shown by desorption spectra b and c of fig. 3 from samples containing 20 and 30% of iron substituted by manganese. The nickel substituted samples on the other hand gave low intensity H_2 desorption profiles as shown by the data of fig. 4 and only two peaks at 625 and 800 K were

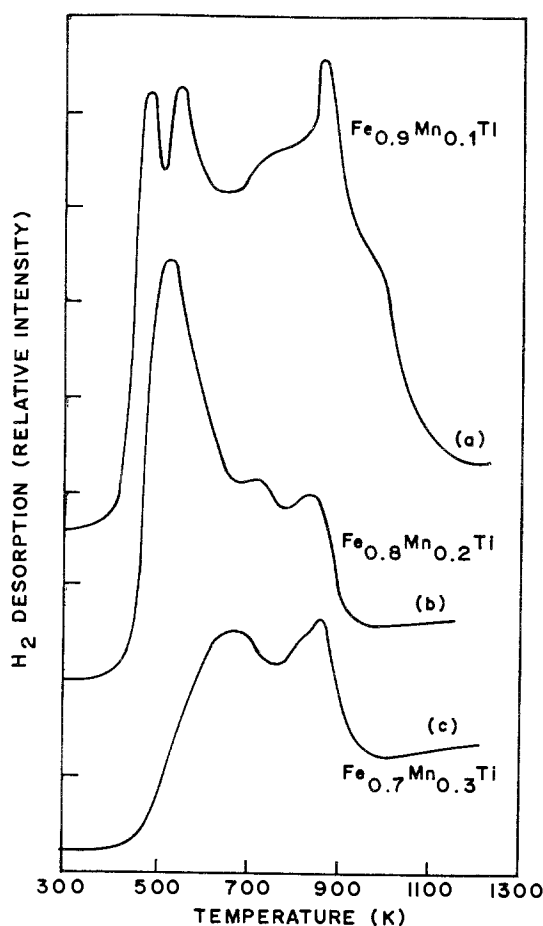


Fig. 3. Hydrogen desorption spectra from $\text{Fe}_{1-x}\text{Mn}_x\text{Ti}$ samples with different Mn contents.

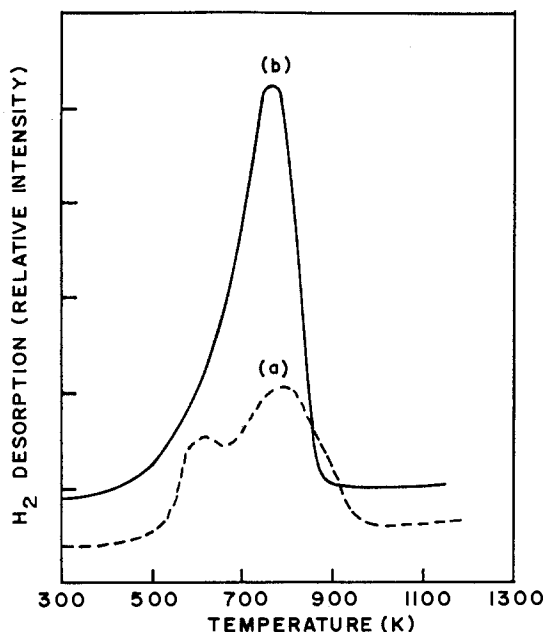


Fig. 4. Hydrogen desorption spectra from $\text{Fe}_{1-x}\text{Ni}_x\text{Ti}$ samples with different Ni contents: (a) $\text{Fe}_{0.9}\text{Ni}_{0.1}\text{Ti}$; (b) $\text{Fe}_{0.6}\text{Ni}_{0.4}\text{Ti}$.

observed. The amount of hydrogen desorbed from manganese and nickel substituted samples under identical test conditions are given in table 1.

4. Discussion

Various views have been expressed on the nature of active sites in Fe-Ti intermetallics responsible to hydrogen dissociation. Existence of super paramagnetic iron clusters below titanium rich outer surface layers have been proposed as active sites by Schalpbach and coworkers [9,10]. Kim and Jai-younglee [11] have suggested that addition of elements with higher oxygen stabilities, such as Mn, Mg, Al or Si promote the H_2 activation process by preserving iron clusters from oxygen contamination. Some authors, on the other hand, emphasize the role of suboxides of iron and titanium existing on the surface of FeTi particularly for titanium rich samples [12,13].

The centres responsible for hydrogen adsorption/storage and giving rise to desorption profiles of figs. 1–4 may belong to the following categories

1. The surface segregated metal iron clusters with different crystallographic faces exposed to adsorbate
2. Fe/TiO_x , Fe/MnO_x or Ti/NiO_x type surface centres
3. FeTiH_n species with hydrogen located at interstitial lattice positions

The data of the present study show that the presence of excess Ti in FeTi or substitution of iron with Mn give rise to additional binding states and to an increased amount of desorbed hydrogen particularly at lower temperatures (figs. 1, 3, table 1). These samples were also found to be more active for the CO methanation reaction as compared to FeTi [1,6]. As Mn is known to be inactive for dissociative chemisorption of H_2 , the segregated iron metal clusters may not be responsible for additional desorption peaks.

X-ray diffraction study has revealed the existence of a small concentration of TiO_x type secondary phases in $FeTi_{1+x}$ samples [1]. The Mössbauer and Auger electron spectroscopy investigations have indicated that the iron clusters responsible to H_2 and CO dissociation are located at the outermost surface of $FeTi_{1.15}$ and are embedded in TiO_x or $FeTiO_y$ type matrix [1,14]. It is important to note that the additional H_2 desorption peaks are observed from samples containing Mn or excess Ti both of which are known to be stable in various oxide forms [15]. On the other hand, the substitution with Ni, having only NiO as a stable oxide, causes little effect on H_2 adstates (fig. 4).

It can thus be concluded that the Fe/TiO_x or Fe/MnO_x type species generated at the intermetallic surface are responsible for hydrogen adsorption and its dissociation. The activation energy (E_a) required for the CO methanation reaction on $FeTi_{1.15}$ has been found to be close to the value reported for Fe/TiO_2 while the corresponding E_a was much higher in the case of FeTi [1]. The existence of iron clusters embedded in oxide matrices of different stoichiometry at the surface are known to give rise to secondary phases and hence to micro-cracks resulting thereby in enhanced surface availability for hydrogen chemisorption [16,17]. The hydrogen adsorption data in table 1 are consistent with these views.

The H_2 desorption parameters in iron single crystals have been widely investigated as has been reviewed recently by Morris et al. [18]. The desorption activation energy (E_d) for chemisorbed hydrogen is found to be in the range of 30–85 $kJ\ mol^{-1}$ depending on the physical form and the face orientation of the iron crystal employed. As the supported iron is likely to have similar activation energy values, it may be argued that the peaks in desorption profiles with T_m less than about 750 K (corresponding $E_d \sim 85\ kJ\ mol^{-1}$) have their origin in hydrogen chemisorption over surface iron sites.

A significant amount of atomic hydrogen is known to be located in the interstitial positions when the intermetallics are activated in hydrogen at an elevated temperature and pressure [9], though the amount of atomic H thus stored on atmospheric pressure activation is rather small [5,19]. The dissolved hydrogen may either be released directly on thermal activation or the hydrogen atoms may diffuse to the surface sites following recombination and release in the molecular form. It is well known that the kinetics of gaseous uptake and release can be accelerated by catalyzing the surface with a metal that dissociates a chemisorbed molecule [20]. The Fe particles at the surface would have the same

effect. Also, the iron particles perched over chemically different surroundings would serve as well dispersed supported metal sites with varying catalytic properties. These sites would accelerate the rate of recombination of atomic hydrogen released from bulk and its subsequent desorption leading thereby to overlapping TDS peaks as observed in our study. On the basis of activation energy values discussed above, it may be concluded that the low temperature TDS peaks arise from associative recombination of H atoms at energetically heterogeneous surface Fe sites. The tailing higher temperature (> 700 K) peaks in the TDS spectra may be assigned to the hydrogen desorbing from the bulk.

References

- [1] R. Sasikala, N.M. Gupta, S.K. Kulshreshtha and R.M. Iyer, *J. Catal.* 107 (1987) 510.
- [2] L. Schlappbach and T. Riesterer, *Appl. Phys.* A32 (1983) 169.
- [3] T. Mizuno and T. Morozumi, *J. Less-Common Met.* 84 (1982) 237.
- [4] A. Seiler, F. Stucki and P. Charpie, *Solid State Commun.* 42 (1982) 337.
- [5] S.K. Kulshreshtha, R. Sasikala, P. Suryanarayana, A.J. Singh and R.M. Iyer, *Mat. Res. Bull.* 23 (1988) 333.
- [6] S.K. Kulshreshtha, R. Sasikala, N.M. Gupta and R.M. Iyer, *J. Catalysis* - communicated.
- [7] V.S. Kamble, N.M. Gupta and R.M. Iyer, *J. Catal.* 113 (1988) 398.
- [8] R.J. Cvetanovic and Y. Amenomiya, *Advan. Catal.* 17 (1967) 103.
- [9] L. Schlappbach, A. Seiler, F. Stucki and H.C. Siegmann, *J. Less-Common Met.* 73 (1980) 145.
- [10] L. Schlappbach, A. Seiler and F. Stucki, *Mat. Res. Bull.* 13 (1978) 697; 1031.
- [11] H.C. Kim and J.Y. Lee, *J. Less-Common Met.* 105 (1985) 247.
- [12] T. Schober and D.G. Westlake, *Scri. Met.* 15 (1981) 913.
- [13] A. Venkert, M.P. Dariel and M. Talianker, *J. Less-Common Met.* 103 (1980) 361.
- [14] N.M. Gupta and S.K. Kulshreshtha, unpublished work.
- [15] *CRC Handbook of Chemistry and Physics*, ed. R.C. Weast (CRC Press, Boca Raton, Fl, 1979) p. B-96.
- [16] H. Zuchner and G. Kirch, *J. Less-Common Met.* 996 (1984) 143.
- [17] P. Selvam, B. Viswanathan, C.S. Swamy and V. Srinivasan, *Int. J. Hydrogen Energy* 12 (1987) 245.
- [18] M.A. Morris, M. Bowker and D.A. King, in: *Comprehensive Chemical Kinetics*, eds. C.H. Bamford, C.F.H. Tipper and R.G. Compton, Vol. 19 (Elsevier, Amsterdam, 1984) p. 1.
- [19] E.L. Huston and G.D. Sandroek, *J. Less-Common Met.* 74 (1985) 435.
- [20] M.W. Ruckman and M. Strongin, *Phys. Rev. B* 29 (1985) 7105.